 doi:10.20944/preprints201804.0039.v1

Article

Examination of Multiband IFA for UHF and SHF Channel Applications

Erfan Rohadi*, Amalia Amalia*, Indrazno Siradjuddin, Ferdian Ronilaya, Rosa Andrie Asmara

Department of Electrical Engineering, State Polytechnic of Malang, Malang, Indonesia;
erfanrohadi@polinema.ac.id (E.R); amalia@polinema.ac.id(A.A); indrazno@polinema.ac.id (I.S),
ferdian@polinema.ac.id (F.R); rosa.andrie@polinema.ac.id (R.A.A)
* Correspondence: erfanr@polinema.ac.id, amalia@polinema.ac.id;

Abstract: The Inverted F Antenna (IFA) with the parasitic element on a finite conducting plane is proposed in the range frequency of 0.1 to 5.5 GHz and its characteristics are analyzed numerically. In this research, the parasitic element and the main IFA are investigated to obtain the resonance frequency for multiband operation purposes. The parasitic element is placed beneath adjusted to the main IFA to derive more frequency bands. The distance between the parasitic element and main horizontal element extremely affects the performance of the IFA. It is found that when the parasitic element is located closer to the conducting plane, this element is coupled by the current on the conducting plane. Consequently, the return loss bandwidth becomes narrower. Therefore, the gain of the proposed IFA becomes a bit higher. The antenna gain is about 8.21 dB at band #3 ($\lambda_{1.747}$), 7.43 dB at band #5 ($\lambda_{2.967}$) and 8.82 dB at band #6 ($\lambda_{4.023}$). This occurs when the calculation condition is antenna height $h1$ = 23 mm, $h2$ = 21 mm, horizontal antenna elements L = 173.2 mm, $L1$ = 140.9 mm and Lp = 152 mm, shorted element Ls = 30.7 mm, the distance between parasitic element and shorted element pyl = 5 mm. While the size of conducting plane is considered pxp+pxm by pyp+pym as 57.5+57.5 mm by 200+50 mm. In the numerical analysis, the electromagnetic simulator WIPL-D based on Method of Moment is used. The results show that the proposed IFA has UHF and SHF channel receiver which are suitable for advanced wireless service (band #3), mobile phones, Bluetooth, maritime service, radiolocation service (band #5) and radars, mobile phones, commercial wireless LAN (band #6).

Keywords: inverted F antenna; near field; radiation pattern; parasitic element; multiband

1. Introduction

The structure of an antenna that has a simple and compact design with low-cost materials and its performance met to the many wireless application systems still becomes the focus of interest for some antenna researchers, especially in bandwidth characteristic enhancement and the ability to operate in multiband. Multiband antenna is an antenna designed to work in multiple bands of frequencies in where one part of the antenna is active for a single band, while another part is active for a different band. Most of the portable devices need to support multiple applications that at one time can be operated. For example, the operation of mobile phones and other mobile devices [1][2]. The one of possibility design that meets those requirements is the low profile inverted F antenna. For the convenience, the inverted F antenna is called IFA in this paper.

The basic of IFA is a variation on the conventional transmission line antenna, or some works determine as a bent monopole antenna (inverted L antenna), with an unbalanced feed point that provides for accommodation of the input impedance matching. The antenna structure solution bears a resemblance to the letter F, face down to the conducting plane [3-6]. Some researchers concluded that the element of inverted F antennas initially evolved from the additional short stub of the folded L antenna [7-9]. Furthermore, the L antenna (or inverted L antenna) can be perceived as a bent monopole or transmission line antenna. The bending of the monopole solutions in a reduced size and

 doi:10.20944/preprints201804.0039.v1

low profile is necessary purpose [10]. For wireless mobile communication systems, the monopole is the most widely used. An array of monopole for all one knows as the most common antenna element for portable equipment, such as mobile phones, conventional cordless devices, vehicles, transportations, etc. [11-13]. Both the inverted L and the proposed IFA have analyzed by using equivalent transmission line terms. Their radiation pattern characteristics in both principal planes are not much different from monopole antenna or transmission line antenna [10].

One of the authors has numerically and experimentally analyzed the ultra-low profile unbalanced fed inverted F antenna for 2.45 GHz Wireless Communication System, and the results show as the base station antenna with return loss bandwidth less than -10 dB and the gain were 3.67% and 4.15 dB, respectively [14]. The previous work of authors has been analyzed numerically by an inverted F antenna for UHF channel at 639 MHz to realize the bandwidth enhancement. The results show the antenna with return loss bandwidth less than -10 dB becomes 2.4 % and the gain becomes 6.58 dB [15].

In this work, the proposed inverted F antenna with the parasitic element on a finite conducting plane examined in the range frequency of 0.1 to 5.5 GHz, and its characteristics are analyzed numerically. The proposed IFA is typically a narrowband antenna that is the disadvantage of this antenna. Therefore, to accomplish the bandwidth enhancement of IFA is by adding the parasitic element. The addition of parasitic elements and by adjusting the height of a vertical element, horizontal element, and the distance between horizontal and parasitic element, the resonance frequency is necessary considered for multiband operation purposes. In the numerical analysis, the electromagnetic simulator WIPL-D based on Method of Moment is used [16-19].

2. Antenna Design and Structure

2.1. IFA Design and Calculation

Firstly, the total length of the proposed IFA must be considered by using the Eq. 1. The Eq. 1 shows the general formulas that can be used to determine the total effective length of IFA, $Ls + L + h$ where h is the height of IFA. The resonance condition then is expressed by following equation (1).

$$Ls + L + h = \frac{\lambda}{4} \tag{1}$$

Where λ is desired wavelength. As $\lambda = \frac{c}{f}$, where f is desired frequency of IFA and c is the speed of light [17]. Thus,

$$f = \frac{c}{4(Ls+L+h)} \tag{2}$$

2.2. IFA Structure

In this proposed design of IFA, the parasitic element added to the antenna structure. The parasitic element is located beneath the horizontal element L and $L1$, and we called it Lp. The main reason for adding the parasitic element is to excite another resonance frequency. Initially, the proposed IFA without parasitic element has been resonated at 639 MHz as reported in this article [15]. Furthermore, the multiband operation achieved when the parasitic element located beneath adjusted to the horizontal element L and $L1$. Figure 1 illustrates the structure of the proposed antenna with the addition of parasitic element, while Table 1 showed the calculation condition of the proposed antenna parameters when the best antenna performances achieved.

In the calculation by using WIPL-D, the height $h1$ of the antenna is adjusted from 23 to 54 mm, and the height of the parasitic element $h2$ is adjusted from 21 to 52 mm corresponds to the distance between main horizontal element of IFA and the parasitic element, while the length Ls of shorted antenna element is adjusted from 15 mm to 31 mm. The length of horizontal elements L, $L1$, and Lp, is adjusted to achieve the input impedance 50 Ω. The size of conducting plane is considered $pxp+pxm$ by $pyp+pym$ as 57.5+57.5 mm by 200+50 mm. The proposed IFA consist of the semi-rigid coaxial cable. The radius of the outer conductor is 1.095 mm, and that of the inner conductor is 0.255 mm. The inner

Preprints (www.preprints.org) | NOT PEER-REVIEWED | Posted: 3 April 2018 doi:10.20944/preprints201804.0039.v1

conductor extended from the end of the outer conductor; this antenna is excited at the end of the outer conductor (feed point). The numerical analysis of the calculation results of the designed IFA optimizes all critical parameters such as return loss bandwidth (-10 dB) at each resonant frequency. In the radiation pattern characteristic examination, both components E_θ and E_ϕ at the x-y plane and y-z plane are analyzed in order to determine the directive gain.

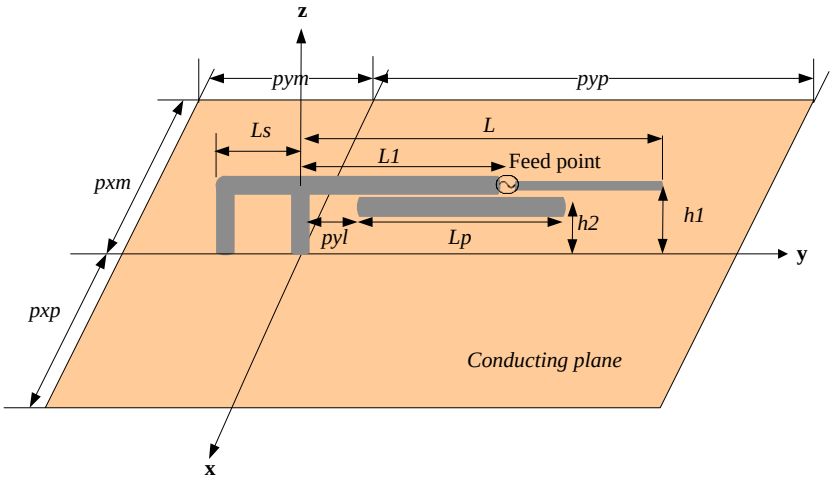

Figure 1. Structure of the proposed IFA

Table 1. Detailed dimensions of the proposed IFA

Parameter	Dimensions [mm]
Ls	30.7
L	173.2
L1	140.9
Lp	152
h1	23
h2	21
pxp	57.5
pxm	57.5
pym	50
pyp	200
pyl	5

3. Results and Discussion

In this section, the calculation results of the proposed IFA performance discussed. This design of the proposed IFA was calculated by using the electromagnetic simulator WIPL-D.

3.1. The Parameters of IFA

It is well-known that the conducting plane size can affect the performance of the antenna. For example [20] it was shown that varying the conducting plane size effects as the result of return loss bandwidth. Some antenna tends to couple strongly to the conducting plane resulting in significant radiation from the conducting plane [2]. Furthermore, the size of conducting plane has been considered as 115 mm by 250 mm. The length of the horizontal element of the main IFA and the parasitic element also give effect to the result of return loss bandwidth. Therefore, the length of the horizontal element of the main IFA and the parasitic element (*L, L1*, and *Lp*) are optimized to get the best result of return loss bandwidth which is greater than -10 dB. Also, the length of the horizontal elements (*L, L1,* and *Lp*) are optimized so that the input impedance matches at the designed frequency. The calculation conditions of other parameters on the proposed IFA such as heights (*h1* and *h2*), short stub (*Ls*) have considered due to examining antenna performances. In this case, the

Preprints (www.preprints.org) | NOT PEER-REVIEWED | Posted: 3 April 2018 doi:10.20944/preprints201804.0039.v1

length of L = 173.2 mm, $L1$ = 140.9 mm, and Lp = 152 mm for all calculation conditions. The simulated result shows that the return loss bandwidth at -10 dB is achieved at all seven resonant frequencies. The maximum return loss which is -51.23 dB is achieved at band #5 as shown in Figure 2.

The heights ($h1$) of IFA investigated at 23 mm, 38.3 mm, and 53.7 mm with the same distance at 2 mm corresponds to the height of the parasitic element ($h2$) are at 21 mm, 36.3 mm, and 51.7 mm. While, the short stubs (Ls) of the proposed IFA adjusted at 15.3 mm, 21.5 mm, 26.1 mm, and 30.7 mm to examine both return loss bandwidth and resonant frequencies.

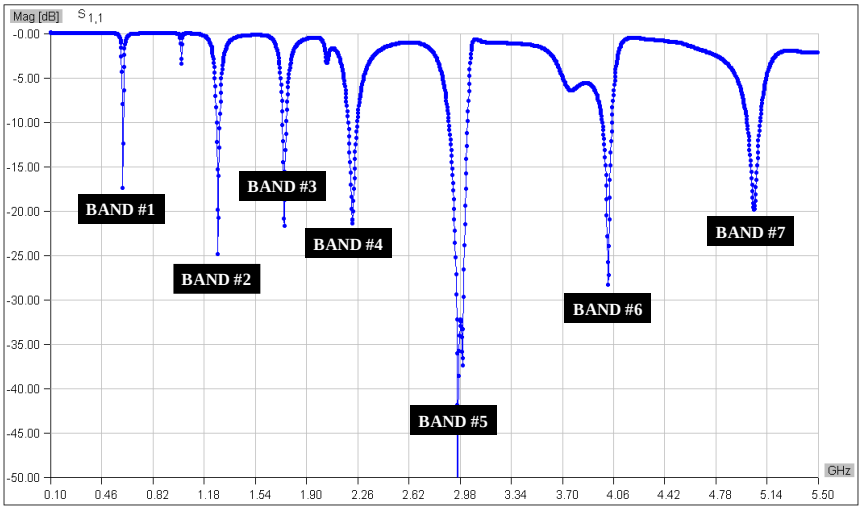

Figure 2. The return loss characteristics of the proposed IFA

3.2. *The Effects of Parasitic Element*

Two significant factors associated with antenna design are the antenna resonant point or center operating frequency and the antenna bandwidth or the frequency range over which the antenna design can work. These two factors are naturally significant features of any antenna design, and as such, they mentioned in specifications for particular antennas. Whether the antenna is used for broadcasting, WLAN, cellular telecommunications, PMR or any other application, the performance of the antenna is paramount, and the antenna resonant frequency and the antenna bandwidth are of great importance [11][12]. The idea of using a parasitic element to increase the bandwidth of an antenna and obtain other resonant frequency well known in antenna theory [21].

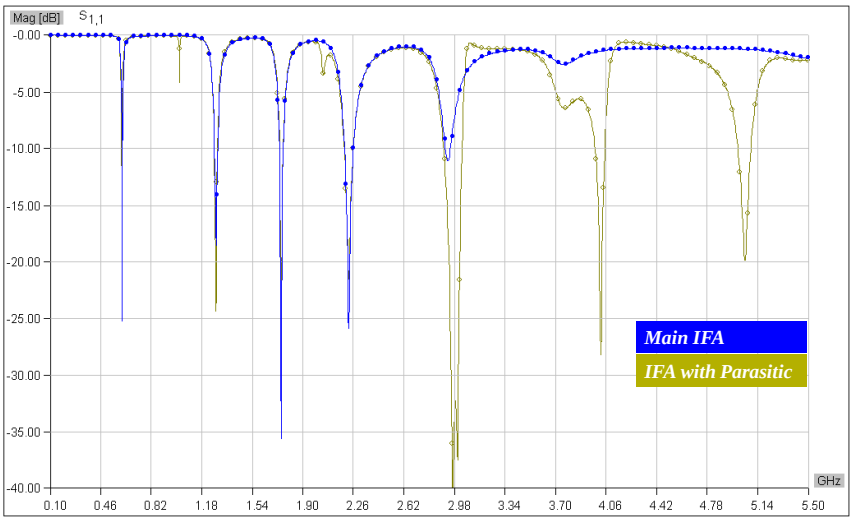

Figure 3. The comparison of the return loss characteristics of the proposed IFA with parasitic

Preprints (www.preprints.org) | NOT PEER-REVIEWED | Posted: 3 April 2018 doi:10.20944/preprints201804.0039.v1

In this work, to obtain multiband IFA, a parasitic element is placed beneath adjusted to the main IFA to derive more frequency bands. The position of the parasitic element is chosen to be close to the conducting plane to achieve 50 Ω impedance matching. The calculation results of the proposed IFA show that both horizontal elements (main element and parasitic element) resonate at seven different frequencies which at 0.61 GHz, 1.27 GHz, 1.74 GHz, 2.22 GHz, 2.96 GHz, 4 GHz and 5 GHz as shown in Table 2. The basic of the proposed IFA without the parasitic element already resonates at five different frequencies. Furthermore, the addition of the parasitic element gave a bit of the bandwidth enhancement as shown in Figure 3. Hence, at the same time, another resonant frequency occurred.

Table 2. Control range of the Bands of the proposed IFA

Band	Center Frequency (GHz)	Control Range at -10 dB (GHz)	Bandwidth at -10 dB (%)
Band #1	0.6103	0.6076 - 0.6157	1.33
Band #2	1.2799	1.2691 - 1.2907	1.69
Band #3	1.747	1.7335 - 1.7605	1.55
Band #4	2.2249	2.1952 - 2.2573	2.79
Band #5	2.9674	2.9026 - 3.0349	4.46
Band #6	4.0231	3.9820 - 4.0501	1.69
Band #7	5.0491	5.0000 - 5.0900	1.78

3.3. *The Height and The Short Stub of IFA*

Variation of the height of the proposed IFA from the conducting plane affects the bandwidth of a few percentage and some resonant frequencies become lower or higher as shown in Figure 4.

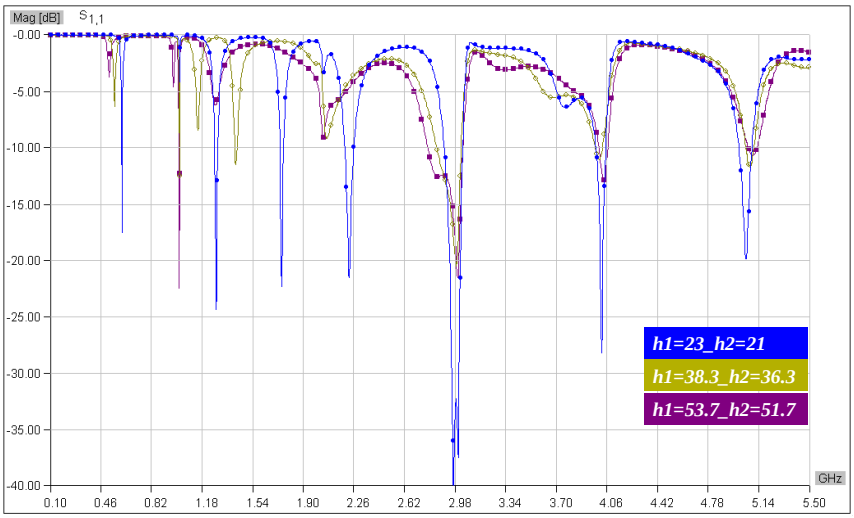

Figure 4. The return loss characteristics of the proposed IFA with different height (h1 and h2)

When the parasitic element located closer to the conducting plane, this element coupled with the current on the conducting plane. Consequently, the return loss bandwidth becomes narrower. Therefore, the gain of the proposed IFA becomes a bit higher. It means that the parasitic element placement must consider very well. This phenomenon is shown in Table 3. In other words, when the parasitic element located quite has distance from conducting plane, it was not working well. Also, the resonant frequencies are not satisfied as the consequent with some lower resonant frequency becomes not available.

Preprints (www.preprints.org) | NOT PEER-REVIEWED | Posted: 3 April 2018 doi:10.20944/preprints201804.0039.v1

Table 3. The return loss bandwidth and gain with different height

Height *h1* (mm)	Height *h2* (mm)	Band	Bandwidth at -10 dB (%)	Gain (dB)
23	21	Band #1	1.33	6.58
		Band #2	1.69	7.51
		Band #3	1.55	8.21
		Band #4	2.79	6.85
		Band #5	4.46	7.43
		Band #6	1.69	8.82
		Band #7	1.78	8.68
38.3	36.3	Band #1	N/A	N/A
		Band #2	N/A	N/A
		Band #3	1.10	5.79
		Band #4	N/A	N/A
		Band #5	5.78	4.50
		Band #6	1.32	6.80
		Band #7	1.18	3.52
53.7	51.7	Band #1	N/A	N/A
		Band #2	N/A	N/A
		Band #3	N/A	N/A
		Band #4	N/A	N/A
		Band #5	8.29	3.20
		Band #6	1.51	2.06
		Band #7	1.17	7.00

The *Ls* adjustments do not significantly affect the bandwidth enhancement of the proposed IFA of band #2, band #3, and band #4 as lower bands as shown in Figure 5. Therefore, the shorter length of *Ls* a bit affects to resonant frequency move to a higher frequency at lower bands. The comparison return loss bandwidth with different *Ls* is shown clearly by the graph in Figure 6.

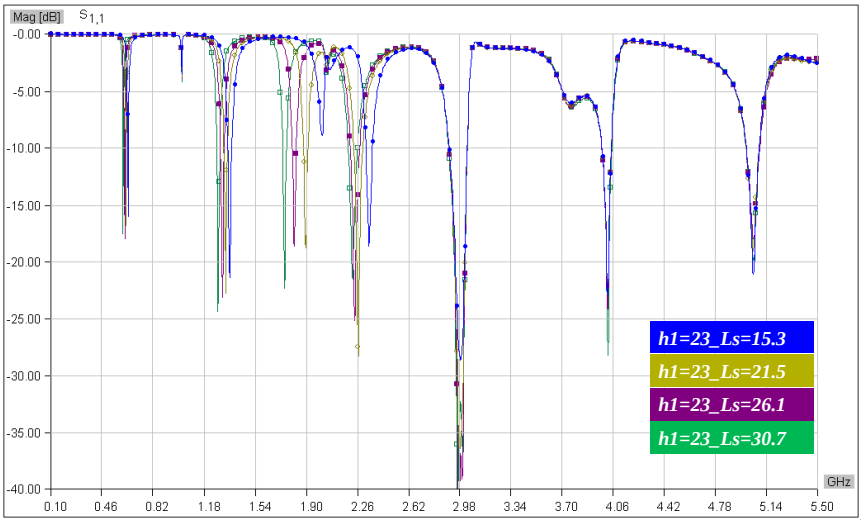

Figure 5. The return loss characteristics of the proposed IFA with different Ls

Preprints (www.preprints.org) | NOT PEER-REVIEWED | Posted: 3 April 2018 doi:10.20944/preprints201804.0039.v1

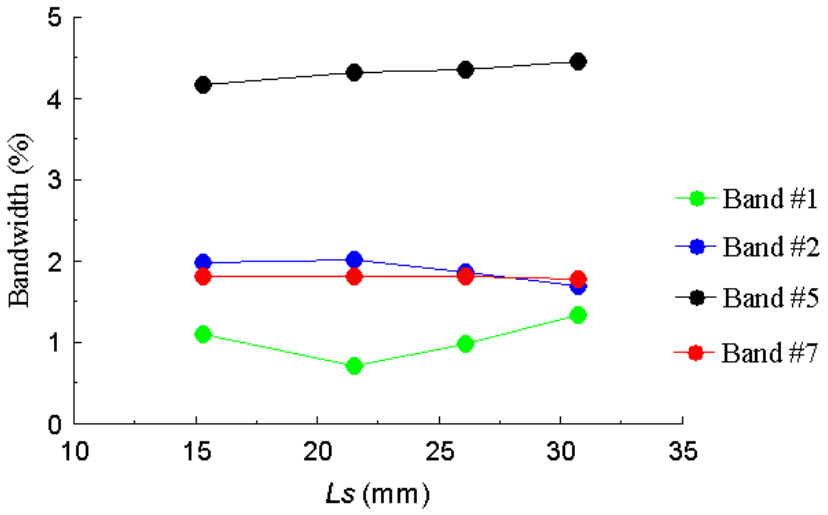

Figure 6. The comparison of the return loss bandwidth with different Ls

3.4. *The Performances of IFA*

The main problem of telecommunication is the phenomenon of conveying information from one point to another. One way to obtain the purpose is using the transmission line media. The communication system will run correctly when the transmission line transmits maximum power or can send power to its full potential. Therefore, the impedance matching between the transmission line loads with the transmission line must consider.

In the transmission line for the communication channel, the problem of impedance matching is a crucial issue, so that the impedance between two media or two related circuits can run properly. Impedance matching or merely matching the portion of a circuit to another is an immensely important part of microwave engineering. Additional circuitry between the two parts of the original circuit may be needed to achieve this matching. This condition occurs when $Z_L \neq Z_0$ where additional circuitry must be located between Z_L and Z_0 to bring the VSWR = 1, or at least approximately [22]. The position of feed point also controls the impedance matching condition. In this proposed IFA, the feed point located between inner and outer conductor due to 50 Ω impedance matching. Figure 7 shows the input impedance characteristic for band #5 and band #6. It obtained by adjusting the horizontal elements (*L, L1, Lp*) and shorted element *Ls* so that the proposed IFA can be called as an antenna with automatic impedance matching.

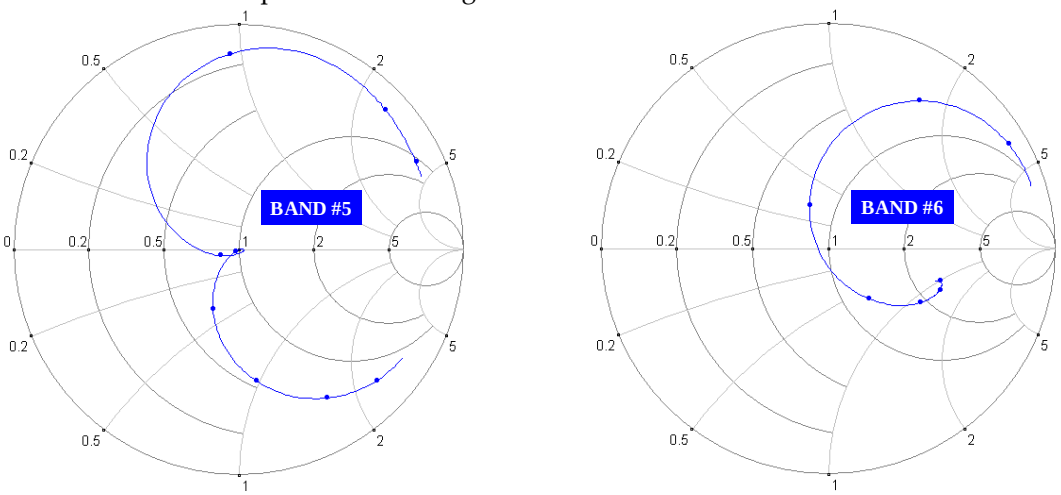

Figure 7. The input impedance characteristics of the proposed IFA (Band #5 and Band #6)

A radiation pattern defines the variation of the power radiated by an antenna as a function of the direction away from the antenna [23]. The energy radiated by the antenna in a particular direction

Preprints (www.preprints.org) | NOT PEER-REVIEWED | Posted: 3 April 2018 doi:10.20944/preprints201804.0039.v1

measured regarding field strength at a point which is a particular distance from the antenna. While the radiation pattern of the antenna is a graph which shows the variation of the actual field strength of the electromagnetic field at all points which are at equal distance from antenna [11]. Figure 8 shows the comparison of simulated total electric field radiation pattern at the x-y plane, x-z plane and y-z plane for three resonant frequencies. Three resonant frequencies have been chosen to show the measured results of the radiation pattern which at 1.74 GHz, 2.96 GHz and 4 GHz. From the radiation pattern characteristics, IFA has a vertical polarization. The maximum gain achieved when the total length of the main horizontal element *L+Ls* was 203.9 mm of band #3.

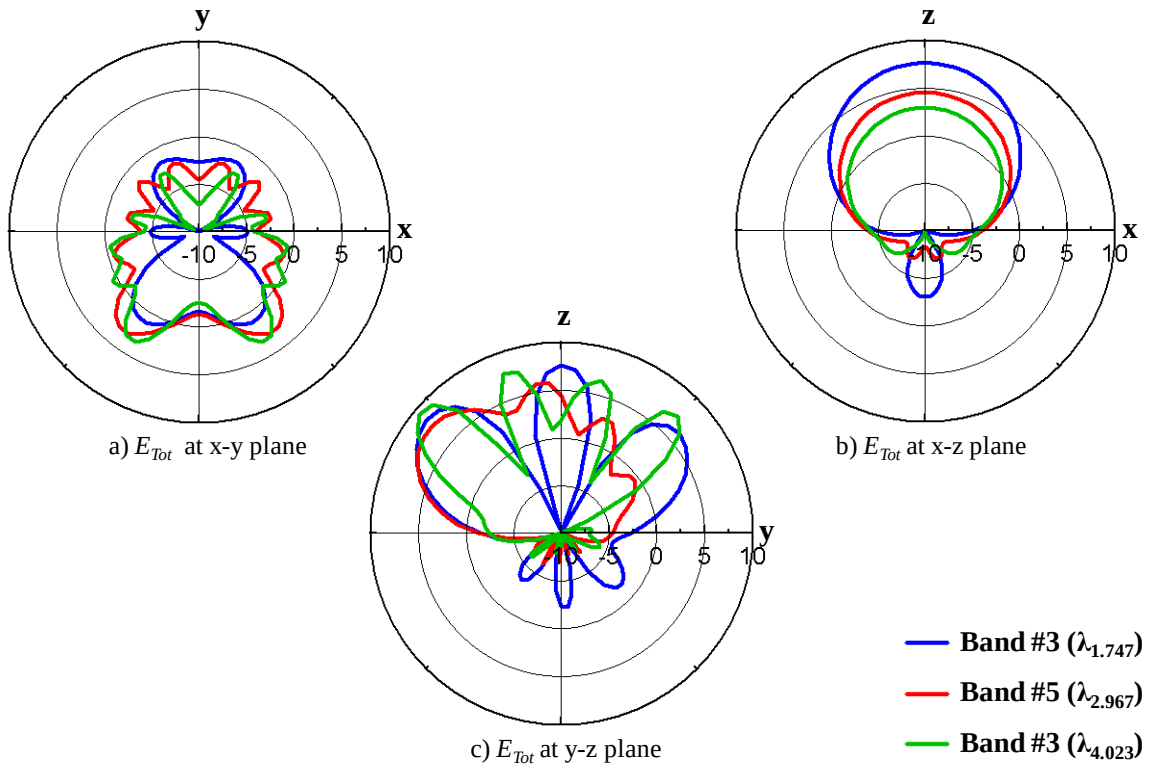

a) E_{Tot} at x-y plane

b) E_{Tot} at x-z plane

c) E_{Tot} at y-z plane

Figure 8. The radiation patterns characteristics of the IFA

The near field is the region of the electromagnetic field (EM) around an object, such as a transmitting antenna or the result of radiation scattering off an object. Non-radiative 'near field' behaviors of electromagnetic fields dominate close to the antenna or scattering object. The importance of near-field ingredient depends on many factors including the antenna size and configuration, distance from the antenna, operating frequency and surrounding media characteristics [24]. Figure 9 shows the near-field distribution of the proposed IFA on conducting plane, parasitic element (*Lp*), main horizontal elements (*L* and *L1*), vertical element and the coaxial cable (vertical and horizontal elements). The calculation condition is antenna height *h1* = 23 mm, *h2* = 21 mm, horizontal antenna elements *L* = 173.2 mm, *L1* = 140.9 mm and *Lp* = 152 mm, shorted element *Ls* = 30.7 mm, the distance between parasitic element and shorted element *pyl* = 5 mm.

Preprints (www.preprints.org) | NOT PEER-REVIEWED | Posted: 3 April 2018 doi:10.20944/preprints201804.0039.v1

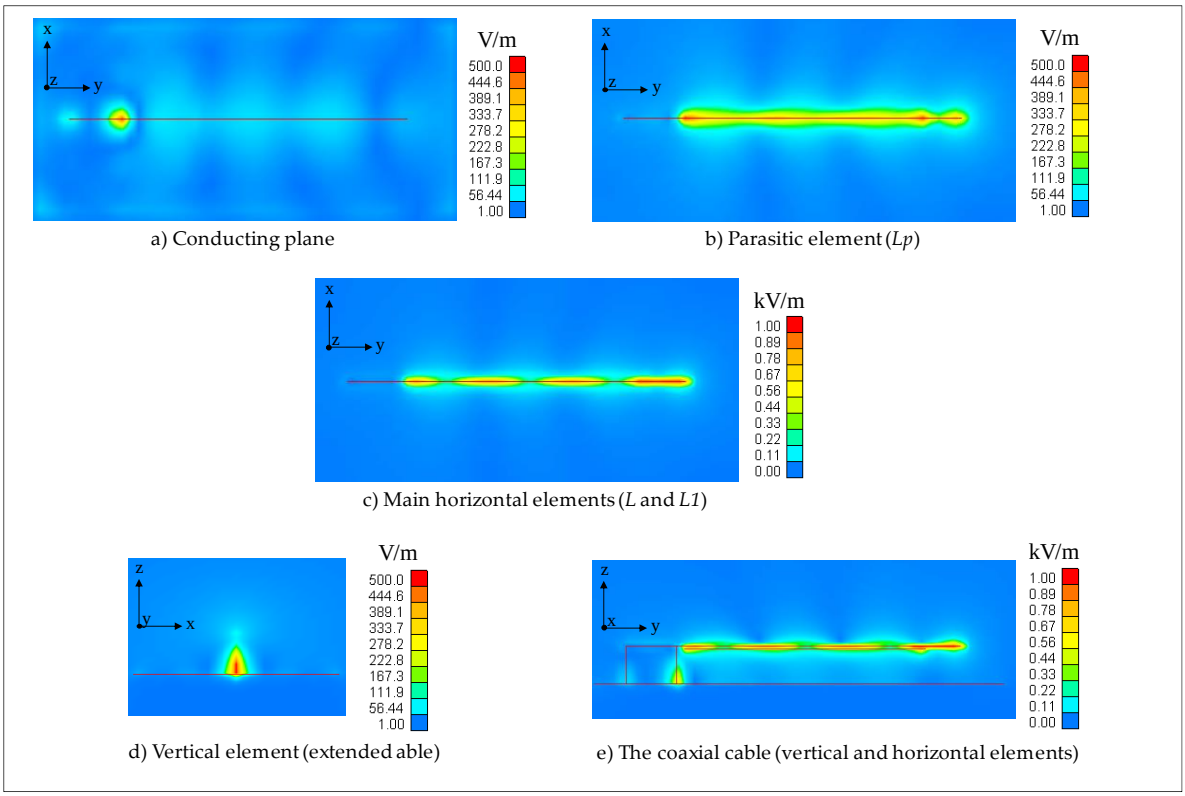

Figure 9. The near-field distribution of the proposed IFA at Band #5

4. Conclusions

The proposed IFA with the parasitic element for multiband antenna application has been presented. By changing some of the key parameters such as the length of the horizontal element (*L*, *L1*, and *Lp*), the height (*h1* and *h2*) and short stub (*Ls*), a multiband IFA is achieved. The distance between the parasitic element and main horizontal element extremely affects the performance of the IFA. It means the current of main the horizontal element corresponds to the current of the parasitic element. The antenna gain is about 8.21 dB at band #3 ($\lambda_{1.747}$), 7.43 dB at band #5 ($\lambda_{2.967}$) and 8.82 dB at band #6 ($\lambda_{4.023}$) when the calculation condition are antenna height *h1* = 23 mm, *h2* = 21 mm, horizontal antenna elements *L* = 173.2 mm, *L1* = 140.9 mm and *Lp* = 152 mm, shorted element *Ls* = 30.7 mm, the distance between parasitic element and shorted element *pyl* = 5 mm and conducting plane size 115 mm by 250 mm. The proposed IFA has UHF and SHF channel receiver which are suitable for advanced wireless service (band #3), mobile phones, Bluetooth, maritime service, radiolocation service (band #5) and radars, mobile phones, commercial wireless LAN (band #6). For the future work, this IFA will be examined experimentally.

Acknowledgments: The authors would like to thank State Polytechnic of Malang for supporting this research.

Author Contributions: This study was led by E.R. while A.A. assisted with the computer simulation and analysis under the supervisions of E.R. and I.S. E.R, A.A., I.S., F.R, and R.A.A wrote the paper.

Conflicts of Interest: The authors declare no conflict of interest.

References

1. Redzwan, F.N.M.; Ali, M.T.; Tan, M.M.; Miswadi, N.F. Design of tri-band Planar Inverted F Antenna (PIFA) with parasitic elements for UMTS2100, LTE and WiMAX mobile applications. In Proceedings of the IEEE 2015 International Conference on Computer, Communications, and Control Technology (I4CT), 21-23 April 2015, pp. 550-554, doi: 10.1109/I4CT.2015.7219639.
2. Abutarboush, H.F.; Nilavalan, R.; Peter, T.; Cheung, S.W. Multiband inverted-F antenna with independent bands for small and slim cellular mobile handsets. *IEEE Transactions on Antennas and Propagation* **2011**, *59(7)*, 2636-2645, doi: 10.1109/TAP.2011.2152350.

3. Gobien III, A.T. Investigation of low profile antenna designs for use in hand-held radios. Doctoral dissertation, Virginia Tech, 1997, pp. 98-103.
4. Kuboyama, H.; Tanaka, Y.; Sato, K.; Fujimoto, K.; Hirasawa, K. Experimental results with mobile antennas having cross-polarization components in urban and rural areas. *IEEE Transactions on Vehicular Technology* **1990**, *39*(2), 150-160, doi: 10.1109/25.54231.
5. Fujimoto, K.; Henderson, A.; Hirasawa, K.; James, J.R. Small Antennas, England: Research Studies Press, 1987.
6. Ogawa, K.; Uwano, T.A diversity antenna for very small 800-MHz band portable telephones. *IEEE Transactions on Antennas and Propagation* **1994**, *42*(9), 1342-1345, doi: 10.1109/8.318664.
7. Fujimoto, T.; Taguri, J. Wideband printed inverted-F antenna with unidirectional radiation pattern. In Proceedings of the IEEE-APS Topical Conference on Antennas and Propagation in Wireless Communications (APWC), 19-23 September 2016, pp. 181-182, doi: 10.1109/APWC.2016.7738151.
8. Fujimoto, T.; Yoshida, T. A printed inverted-F antenna for circular polarization. In Proceedings of the IEEE International Symposium on Antennas and Propagation (APSURSI), 26 June-1 July 2016, pp. 2171-2172, doi: 10.1109/APS.2016.7696792.
9. Saita, Y.; Ito, T.; Michishita, N.; Morishita, H. Low-frequency inverted-F antenna on hemispherical ground plane. In Proceedings of the IEEE International Symposium on Antennas and Propagation (ISAP), 2-5 December 2014, pp. 183-184, doi: 10.1109/ISANP.2014.7026591.
10. Nikolova, N.K. Lecture 10: Other Practical Dipole/Monopole Geometries Matching Techniques for Dipole/Monopole Feeds, Department of Electrical and Computer Engineering, ITB/A308 McMaster University, pp. 15-16, 2003.
11. Ballanis, C.A. *Antenna theory analysis and design,* 4th ed.; John Willey and Son's Inc: New York, NY, USA, 1997; pp. 151-184, ISBN: 978-1118642061.
12. Stutzman, W.L.; Thiele, G.A. *Antenna theory and design*, 3rd ed.; John Willey and Son's Inc: New York, NY, USA, 2012; pp. 229-235, ISBN: 978-0-470-57664-9.
13. Sinnema, W. *Electronic Transmission Technology;* Prentice Hall Inc.: Englewood Cliffs, New Jersey, USA, 1988; pp. 112-118, ISBN: 0132522217.
14. Rohadi, E.; Taguchi, M. Ultra-low profile, unbalanced fed inverted F antenna for 2.45 GHz wireless communication system. In Proceedings of the IEEE URSI International Symposium on Electromagnetic Theory (EMTS), 20-24 May 2013, pp. 585-588.
15. Rohadi, E.; Amalia; Siradjuddin, I. Numerical Analysis of The Bandwidth Enhancement of an Inverted F Antenna for UHF Channel at 639 MHz. In Proceedings of the 15th International Conference on Quality in Research (QiR), 24-27 July 2017, pp. 549-552.
16. Milligan, T.A. *Modern antenna design,* 2nd ed.; John Willey and Son's Inc: New York, NY, USA, 2005; pp. 67-72, ISBN: 978-0-471-45776-3.
17. Shao, J. *Mathematical Statistic,* 2nd ed.; Springer-Verlag New York: New York, NY, USA, 2003; pp. 207-212, ISBN. 978-0-387-21718-5.
18. Kolundžija, B.M.; Sumić, D.S.; Sarkar, T.K.; Ognjanovic, J.S. *WIPL-D Microwave: Circuit and 3D EM Simulation for RF & Microwave Applications: Software and User's Manual*. WIPL-D.; Artech House, Inc: Norwood, MA, USA, 2005, ISBN. 86-86173-00-4.
19. Khan, N. Design of planar Inverted-F antenna. In Proceedings of the International Journal of Advanced Technology in Engineering and Science **2014**, *2(5)*, pp. 20-31.
20. Abedin, M.F.; Ali, M. Modifying the ground plane and its effect on planar inverted-F antennas (PIFAs) for mobile phone handsets. *IEEE Antennas and Wireless Propagation Letters* **2003**, *2*(1), 226-229, doi: 10.1109/LAWP.2003.819669.
21. Stoiljkovic, V.; Wilson, G. A small planar inverted-F antenna with parasitic element for WLAN applications. In Proceedings of the IEEE Tenth International Conference on Antennas and Propagation, (Conf. Publ. No. 436), 14-17 April 1997, pp. 82-85, doi: 10.1049/cp:19970213.
22. Whites, K.W. Transmission Line Matching Using Lumped L Networks; Department of Electrical and Computer Engineering, The South Dakota School of Mines and Technology: Rapid City, South Dakota, USA, 2011, pp. 1-11.
23. Abdullah, M.W.; Fafoutis, X.; Klemm, M.; Hilton, G. S. Radiation Pattern Analysis of Single and Multi-Antenna Wearable Systems. In Proceedings of the IEEE 84th Vehicular Technology Conference (VTC-Fall), 18-21 September 2016, pp. 1-5, doi: 10.1109/VTCFall.2016.7881186.

24. M. Haridim, A. Tsaliovich, J. Gavan, and T. Razban, "Radiating Antenna Near/Far Field Distribution and Region Boundaries", *IEEE Conference on Antenna Measurements & Applications (CAMA),* pp. 1-4, 2016

Haridim, M.; Tsaliovich, A.; Gavan, J.; Razban, T. Radiating antenna near/far field distribution and region boundaries. In Proceedings of the IEEE Conference on Antenna Measurements & Applications (CAMA), 23-27 October 2016, pp. 1-4, doi: 10.1109/CAMA.2016.7815748.